Green and sustainable method of manufacturing anti-fouling zwitterionic polymers-modified poly(vinyl chloride) ultrafiltration membranes

Green and sustainable method of manufacturing anti-fouling zwitterionic polymers-modified poly(vinyl chloride) ultrafiltration membranes

Wancen Xie [a,b], *Alberto Tiraferri* [c], *Xuanyu Ji* [a,b], *Chen Chen* [d], *Yuhua Bai* [e], *John C. Crittenden* [f], *and Baicang Liu* [*,a,b]

[a] Key Laboratory of Deep Earth Science and Engineering (Ministry of Education), College of Architecture and Environment, Institute of New Energy and Low-Carbon Technology, Sichuan University, Chengdu 610207, PR China

[b] Yibin Institute of Industrial Technology, Sichuan University Yibin Park, Yibin, 644000, PR China

[c] Department of Environment, Land and Infrastructure Engineering, Politecnico di Torino, Corso Duca degli Abruzzi 24, 10129 Turin, Italy

[d] Litree Purifying Technology Co., Ltd, Haikou, Hainan 571126, PR China

[e] Infrastructure Construction Department, Chengdu University, Chengdu 610106 PR China

[*] Corresponding author.

E-mail: bcliu@scu.edu.cn; Tel: +86-28-85995998; Fax: +86-28-62138325.

[f] Brook Byers Institute for Sustainable Systems, School of Civil and Environmental Engineering, Georgia Institute of Technology, Atlanta, GA 30332, USA

Abstract

The nonsolvent induced phase separation (NIPS) method for ultrafiltration (UF) membrane fabrication relies on the extensive use of traditional solvents and toxic chemicals, thus ranking first in terms of ecological impacts among all the membrane fabrication steps. Methyl-5-(dimethylamino)-2-methyl-5-oxopentanoate (PolarClean), as a green solvent, was utilized in this study to fabricate poly(vinyl chloride) (PVC) UF membranes. Subsequently, in post-treatment process, a zwitterionic polymer, [2-(methacryloyloxy) ethyl] dimethyl-(3-sulfopropyl) ammonium hydroxide (DMAPS), was grafted onto the membrane surface to enhance its anti-fouling properties. This step was achieved using a surface-initiated activator regenerated by electron transfer-atom transfer radical polymerization (ARGET-ATRP) reaction, with a greener activator compared to traditional ones. This novel method used low toxicity chemicals, thus avoiding the environmental hazards of traditional ATRP and greatly improving the reaction efficiency. We systematically studied the grafting time effect on the resulted membranes using sodium alginate as the foulant, and found that short grafting time (30 minutes) achieved excellent membrane performance: pure water permeability of 2872 L m^{-2} h^{-1} bar^{-1}, flux recovery ratio of 86.4 % after 7-hour fouling test, and foulant rejection of 96.0 %. This work discusses for the first time an approach with low environmental impacts to both fabricate and modify PVC UF membranes.

Keywords

Poly(vinyl chloride) PVC; Ultrafiltration; Green solvent; ARGET-ATRP; DMAPS

1. Introduction

Poly(vinyl chloride) (PVC), the second largest manufactured resin by volume worldwide [1, 2], is also one of the most common polymers applied to fabricate ultrafiltration (UF) membranes due to numerous characteristics (*e.g.*, low-cost, suitable mechanical strength, and acid-alkali-microbial resistance [3-6]). Unfortunately, the intrinsic hydrophobic properties of PVC increase the likelihood of membrane contamination [4, 7], leading to low flux and reduced life-time. This mechanism limits PVC application in the membrane field. To improve the antifouling property of PVC membranes, hydrophilic enhancement is essential [8].

Blending [9-11], surface grafting [12-14], and surface coating [15] are typical modification strategies to improve the hydrophilicity of membranes. Blending entails adding hydrophilic materials during the membrane casting process. Blending is a convenient method, but not without important restrictions: adequate solubility of the additives in the solvent is required [16], and complete coverage of the membrane surface with the additives is usually difficult to achieve [17, 18]. As for surface grafting, this procedure allows the formation of consistent hydrophilic layers on membrane surfaces, as well as the preservation of membrane physical properties [17]. A considerable number of hydrophilic polymers have been studied for grafting purposes and the feasibility of this method has been widely discussed. The literature contains reports on poly(vinylidene fluoride) (PVDF) [19, 20], polyethersulfone (PESU) [21], polysulfone (PSU) [22], and cellulose-based membranes [12, 23] modified via surface grafting by atom transfer radical polymerization (ATRP) reaction. For PVDF membranes, the typical steps include grafting hydrophilic polymers on membrane surfaces pre-coated with biophenols (*e.g.*, polydopamine, tannic acid), which provide active sites for the reaction [17, 19]. However, this approach reduces the permeability of UF membranes due the pore occlusion [24, 25]. Therefore,

direct grafting of hydrophilic materials to the membrane surface may be a better option for which it is possible to exploit the halogen atoms present in the membrane backbones (*e.g.*, PVDF and PVC membranes).

To the best of our knowledge, only a few works have attempted direct grafting of hydrophilic materials to the PVC membrane surfaces [16, 26-29]. Cheng *et al.* [16] grafted poly(2-hydroxyethylmethacrylate) (PHEMA) and poly(1-butyl-3-vinylimidazolium bromide) (PBVIm-Br) on PVC membrane via a 2-step ATRP reaction. This modification method was time-consuming, because for each ATRP step takes at least six hours. moreover, various different chemicals were used in the polymerization process, involving toxic ones. However, the resulting membrane showed low pure water flux (~ 100 $L/m^2 \cdot h$) and unsatisfactory anti-fouling properties (flux recovery ratio of 79.7% after only 100-min fouling test). Other works included hydrophilic materials such as N-vinyl-2-pyrrolidinone (NVP) [26], ethylenediamine (EDA), diethylenetriamine (DETA), pentaethylenehexamine (PEHA) [28], and poly(3-sulfopropyl methacrylate–methacrylatoethyl trimethyl ammoniumchloride–glycidyl methacrylate) (PSTG) [29]. There is no doubt that more work should be done to investigate more efficient materials for the surface grafting of PVC membranes via greener modification strategies.

Zwitterionic polymers have attracted great attention in recent years as modification materials, owing to their hydrophilicity, blood compatibility, and environmental stability [23, 30, 31]. These polymers are composed by the same number of cationic and anionic groups, thus displaying overall neutral potential, and promote a hydration layer around the brushes to significantly reduce membrane fouling [17, 31]. Among zwitterionic polymers, [2-(methacryloyloxy) ethyl] dimethyl-(3-sulfopropyl) ammonium hydroxide (DMAPS) was studied by Zhou *et al.* [32] and was found to be the best performing one in terms of antifouling ability

among 66 monomers used to modify PESU membranes. In addition, DMAPS does not pose dangersto human health and to the environment according to Safety Data Sheet, thus conforming to the principles of green chemistry [33]. There have been works on poly(vinylidene fluoride) (PVDF) [17, 19, 34], polysulfone (PSU) [22], PESU [21], aliphatic polyketone (PK) [35], regenerated cellulose (RC) [36], and poly(lactic acid) (PLA) membranes [37], as well as aromatic polyamide reverse osmosis (RO) membranes [38] and thin-film composite (TFC) forward osmosis (FO) membranes [39] modified by grafting DMAPS, all of which demonstrated improved antifouling properties. However, no PVC membrane has been modified with this molecule, implying a significant deficiency in the field.

The activator regenerated by electron transfer-atom transfer radical polymerization (ARGET-ATRP) reaction is the recent development of ATRP [40], and it can be used to graft polymer brushes to the membrane surface. Our previous studies [9, 41, 42] utilized traditional ATRP to obtain copolymer PVC-g-graft-poly(ethylene glycol) methyl ether methacrylate (PVC-g-PEGMA), which needed alkyl halide (-Cl) ligand and a relatively high concentration of a transition metal catalyst at lower oxidation state (Cu^{I}) to initiate the reaction. In such reaction process, the oxygen must be carefully removed, and high temperature and long polymerization times are required. To avoid these limitations, ARGET-ATRP may be adopted, in which the catalyst is continuously regenerated by a reducing agent from Cu^{II} species [40, 43, 44]. Therefore, only ppm levels of the catalysts are required, and a limited amount of air can be present. Meanwhile, more active ligands can improve the efficiency of the polymerization system, allowing the reaction at room temperature with shortened reaction time [45, 46]. Therefore, ARGET-ATRP is considered a grafting method with lower environmental impacts. [40, 43, 44].

When PVC membranes are prepared via NIPS process, large amounts of organic solvents (*e.g.*, 1-methyl-2-pyrrolidinone) are needed, which are toxic to human and the environment [47-49], thus violating the principles of green chemistry [50-53]. Therefore, green and sustainable solvents are urgently needed to replace traditional ones [54]. Our previous study [55] used PolarClean for PVC membrane fabrication. This compound has no health hazards, and much lower environmental impacts compared to other common membrane preparation solvents [56-61]. Additionally, it is nonflammable and improves the saftey of the whole membrane fabrication process [62, 63]. The PVC membrane prepared by PolarClean in the previous study had ultrahigh pure water permeability and sodium alginate (SA) rejection, but the antifouling property was relatively poor (flux recovery ratio of 57 % after a 7-hour fouling test) [55]. Therefore, in the present work, PolarClean was also utilized to prepare PVC membranes, but we significantly improved the environmental compatibility of the fabrication process as well as improved the antifouling properties of the membranes by grafting DMAPS monomers using sustainable ARGET-ATRP method (Fig. 1). The reaction conditions are investigated and optimized to obtain widely applicable PVC membranes with all-round high performance.

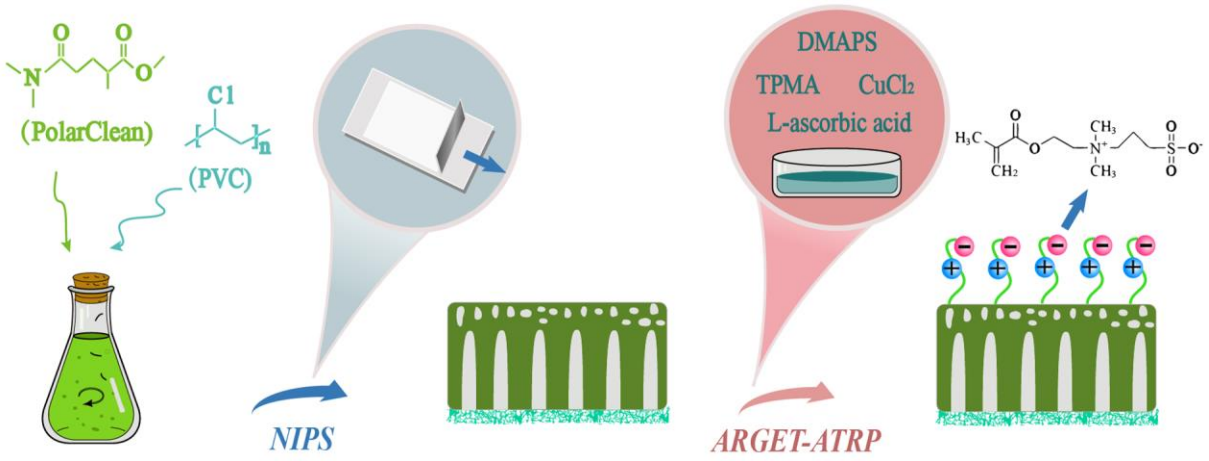

Fig. 1. Schematic overview of the membrane fabrication strategy: dissolution of PVC in green solvent PolarClean, followed by fabrication the virgin membrane via NIPS method. Finally, DMAPS polymers were grafted on the membrane surface via ARGET ATRP method.

2. Materials and methods

2.1. Chemicals

Poly(vinyl chloride) (PVC, high molecular weight), [2-(Methacryloyloxy)ethyl]dimethyl-(3-sulfopropyl)ammonium hydroxide (DMAPS, 95%, Mn = 279.35 g/mol), tris(2-pyridylmethyl)amine (TPMA, 98%), copper (II) chloride ($CuCl_2$, ≥ 99.999%), L-ascorbic acid (> 99%), methanol (99.9 %), sodium chloride (NaCl, reagent grade, 99%), and sodium alginate (SA, Lot# MKBL7997V) were obtained from MilliporeSigma (St. Louis, MO, USA). Ethanol (99.7%) was obtained from Chengdu Chron Chemicals Co., Ltd. (Chengdu, China). PolarClean (> 99.9%) was obtained from Solvay Specialty Polymers (Shanghai, China).

2.2. Preparation of PVC membranes based on PolarClean

The membrane casting solution consisted of a solution of polymer PVC (8 g) and solvent PolarClean (92 g). The membranes were fabricated via NIPS method. Poly(ethylene terephthalate) (PET) non-woven fabric was used as the backing layer. Detailed steps are presented in Text S1 (Supporting Information, SI). The PVC membranes were washed with ethanol to remove the residual solvent, and washed with deionized (DI) water to eliminate ethanol, and stored in DI water at 4 ℃.

2.3. Surface grafting of zwitterionic polymers

Because of the light sensitivity property of L-ascorbic acid, TPMA and $CuCl_2$, the reaction was proceeded in a dark environment. 15.64 g of DMAPS monomer was dissolved in 200 mL of methanol-DI water solution (1:1 v/v) in a 1000 mL sealed glass bottle. After a 10-min nitrogen gas bubbling, 0.004 g of $CuCl_2$ and 0.056 g of TPMA dissolved in a 8 mL of methanol-DI water mixture (1:1 v/v) were added to the solution. Another 10 min N_2 bubbling was applied. The PVC membrane previously secured to a glass sheet with waterproof tape was then placed in the glass bottle, with additional 10 min N_2 bubbling to remove the oxygen in this system. Subsequently, 1.2 g of L-ascorbic acid in 12 mL of methanol-DI water mixture (1:1 v/v) was poured to initiate the reaction. Meanwhile, N_2 was continuously bubbled to stir the solution and remove oxygen. After a designated time (30, 60, or 90 min), the bottle was open to air, and the reaction terminated. Finally, the modified membrane was thoroughly rinsed and stored in DI water at 4 ℃. The labels for pristine membrane and membranes fabricated with 30, 60, 90 min grafting times are M1-0 min, M2-30 min, M3-60 min, and M4-90 min, respectively.

2.4. Ternary phase diagram determination

The cloud points for the PVC-PolarClean system were measured by titration. Different amounts of PVC (6 wt.%, 8 wt.% and 10 wt.%) were completely dissolved in PolarClean, and DI water was slowly added to the solutions at 60 ℃, stirring at 500 rpm, until the solution was no longer homogeneous. As a comparison, the cloud points of PVC-DMAc and PVC-NMP systems were also measured. The results are presented in Figure S1 (SI).

2.5. Membrane surface characterizations

The membrane morphologies were obtained by scanning electron microscopy (SEM) (REGULUS 8230, Hitachi, Japan). The surface roughness was detected by atomic force microscopy (AFM, Dimension Icon, Bruker, Germany), performed in ScanAsyst mode. The

chemical composition for all membranes was gotten by X-ray photoelectron spectroscopy (XPS) (Axis Supra, Kratos Analytical Ltd., UK) and fourier transform infrared (FTIR) spectrometer (Nicolet is 20, Thermo Fisher Scientific Inc., US) with an attenuated total reflection (ATR) equipment [64]. The dynamic water contact angles were measured via a KRÜSS DSA 25S measurement (KRÜSS GmbH, Germany) at room temperature. For more details, the reader can refer to our previous study [55] and Text S2 (SI).

2.6. Ultrafiltration and anti-fouling performance assessment

The membrane filtration tests were conducted using a dead-end filtration cell (Amicon 8200, Millipore, USA), which had an effective membrane area of 28.7 cm^2. The pressure was set at 10 psi (0.07 MPa) to conduct the tests. The permeate was weighed and recorded using a balance (Pro Balance AV8101, Ohaus Adventurer, USA) and Collect 6.1 software every minute. The temperature was 25 ℃ for all the tests. The detailed steps can be found in our previous study [65, 66], and are in Text S3 (SI).

The Shimadzu total organic carbon (TOC) analyzer (Shimadzu Co., Japan) was used to measure the SA concentrations [41]. Meanwhile, the antifouling property of the membrane was characterized by the following indexes: the flux recovery ratio (FRR), the total flux decline ratio (DR_t), the reversible flux decline ratio (DR_r), and the irreversible flux decline ratio (DR_{ir}) [67].

$$FRR=\frac{J_2}{J_1}\times 100\% \quad (1)$$

$$DR_t=\left(1-\frac{J_p}{J_1}\right)\times 100\% \quad (2)$$

$$DR_r=\frac{J_2-J_p}{J_1}\times 100\% \quad (3)$$

$$DR_{ir}=\left(1-\frac{J_2}{J_1}\right)\times 100\% \quad (4)$$

J_1, J_2, J_p (L m^{-2} h^{-1}) are the pure water flux of new membrane, the pure water flux of the membrane after physical cleaning, and the SA solution flux, respectively.

2.7. XDLVO theory to assess the membrane fouling potential

The membrane anti-fouling properties can also be assessed by estimation of the interfacial free energy by the extended Derjaguin, Landau, Verwey and Overbeek (XDLVO) theory, which has been widely used for the foulant-membrane interaction energy calculation, related to the fouling potential of membranes. The total interaction free energy between foulants (denoted with subscript 1) and membrane surface (subscript 2) in a medium (DI water, subscript 3) is obtained by the combination of Lifshitz−van der Waals (LW) and Lewis acid−base (AB) interaction energies [68]:

$$\Delta G_{132}=\Delta G_{132}^{LW}+\Delta G_{132}^{AB} \quad (5)$$

$$\Delta G_{132}^{LW}=-2(\sqrt{\gamma_2^{LW}}-\sqrt{\gamma_3^{LW}})(\sqrt{\gamma_1^{LW}}-\sqrt{\gamma_3^{LW}}) \quad (6)$$

$$\Delta G_{132}^{AB}=2\left[(\sqrt{\gamma_3^+}(\sqrt{\gamma_1^-}+\sqrt{\gamma_2^-}-\sqrt{\gamma_3^-})+\sqrt{\gamma_3^-}(\sqrt{\gamma_1^+}+\sqrt{\gamma_2^+}-\sqrt{\gamma_3^+})-(\sqrt{\gamma_1^+\gamma_2^-}+\sqrt{\gamma_1^-\gamma_2^+})\right] \quad (7)$$

where γ^{LW}, γ^+ and γ^- are the Lifshitze van der Waals, electron acceptor, and electron donor components of membrane surface tension parameters, respectively. These parameter were obtained by contact angle measurements of membranes and foulants, using three probe liquids of known surface tension parameters (water, diiodomethane, and formamide in Table S1) [69, 70]; the calculation details are listed in Table S2 and Text S4 (SI). The electrostatic force (EL)

interaction energy (ΔG_{132}^{EL}) is also one component of the total interaction free energy, but it is much smaller than ΔG_{132}^{LW} and ΔG_{132}^{AB}, and can thus be neglected.

3. Results and discussion

3.1. Membrane morphology

The surface and cross-sectional morphologies for M1-0 min, M2-30 min, M3-60 min, and M4-90 min are reported in Fig. 2A. Based on surface SEM images, it is obvious that the pore diameter and pore density were reduced with the increase of the grafting time. We used Image Pro Plus V.7.0 software (Media Cybernetics, USA) to quantify the pore diameter information and surface porosities (Fig. 2B), as well as maximum pore diameters and pore densities reported in Table S3 (SI). At least two different areas of the same membrane were included for the statistics. The average pore diameters decreased from 18.7 nm for M1-0 min to 12.6 nm for M4-90 min, along with significant reduction of surface porosities from 4.29 % for M1 to 0.49 % for M4. The gradual decrease of pore diameter and surface porosity was attributed to higher DMAPS brush thickness and grafting density resulting from longer ARGET ATRP reaction time. This phenomenon is consistent with previous reports [17, 22, 71]. This phenomenon will reduce the permeabilities of the membranes to some extent, which is discussed below. However, by prolonging the grafting time from 120 min to 180 min, the pore size and porosity did significantly decrease (Fig. S2, SI), which is probably due to the saturation of active sites. The cross-sectional SEM images revealed that this modification method had little effect on cross-sectional pore structure. The 3D AFM images and root-mean-square (R_q) roughness values are shown in Fig. 2A,C. Overall, zwitterionic polymer brushes increased the surface roughness due to relatively uneven DMAPS layers covering the membrane surface [19]. Moreover, some

outshoots, which were formed by the aggregation of the grafted polymer chains, appeared on the surfaces, thus further increasing the surface roughness [22].

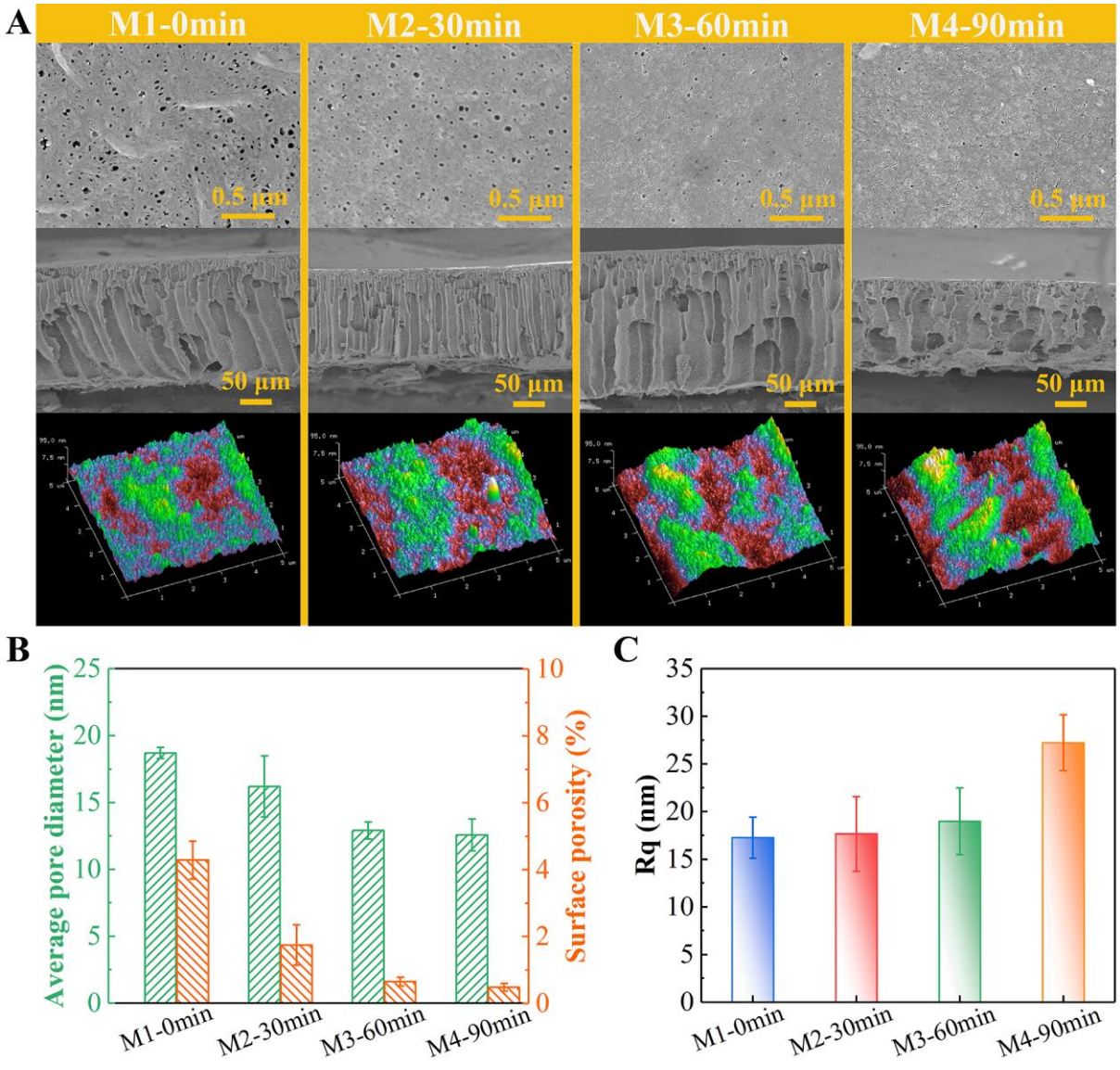

Fig. 2. Membrane morphology. (A) Surface and cross-sectional SEM images, as well as 3D AFM images, of PVC membranes obtained with different grafting times: M1-0 min, M2-30 min, M3-60 min, and M4-90 min. All surface SEM images were under 50K× magnification, and the cross-sectional images under 300× magnification. (B) Average pore diameters and surface porosities of M1-M4. At least two surface SEM images were analyzed for each membrane

sample to obtain these values. (C) R_q surface roughness values of M1-M4 calculated from AFM images. For each membrane sample, at least four different locations on the surface were probed.

3.2. Membrane surface chemistry

The XPS spectra of all membranes are presented in Fig. S3 (SI). For pure PVC membrane, carbon (C) and chlorine (Cl) were the dominant elements on the surface. The low content of oxygen (O) (0.5 At. %) found on the membranes is attributed to the adsorption of H_2O or negligible residues of PolarClean [72]. However, after DMAPS was grafted to membrane surface, new peaks of O, nitrogen (N) and sulfur (S) were detected. We used CasaXPS processing software (Casa Software Ltd., U.K.) to estimate element atom percentages for M1-M4, with the results summarized in Table 1. Moreover, this software was also employed to carry out C 1s peak curve-fitting, and the results are shown in Fig. 3A-D. Specifically, for M1-0 min, only C-C/C-H (284.6 eV) and CHCl (285.7 eV) peaks were observed. However, after surface grafting, peaks attributed to C-N/C-O/C-S (286.4 eV) and O-C=O (288.2 eV) appeared, proving the successful grafting of DMAPS to the surfaces. As DMAPS polymers were the only source of O-C=O, the mole fraction of DMAPS can be estimated using eq. (8) [14, 66]:

$$X^{DMAPS} = \frac{A_{COO}}{A_{COO} + A_{CHCl}} \quad (8)$$

A_{CHCl} and A_{COO} represent the areas of CHCl and COO peaks, and corresponding results are also reported in Table 1. Compared to our previous study, which entailed the modification of PVC membranes by blending hydrophilic polymers with PVC in the casting solution [55], this grafting method was much more efficient to introduce more zwitterionic polymers on the surface, which is an important feature to achieve anti-fouling performance (*vide infra*). The content of DMAPS

277 at the near-surface of membranes increased with increasing grafting time, indicating higher
278 grafting density and ticker brushes. Fig. 3E reports the ATR-FTIR spectra of all membranes.
279 After polymerization, new bonds at 3363 cm^{-1}, 1727 cm^{-1}, and 1039 cm^{-1} appeared, which are
280 associated to quaternary ammonium, C=O, and -SO_3 groups, thus indicating the successful
281 grafting of DMAPS on the surfaces of M2-M4.

282 **Table 1.** Element atom percentages and mole fraction of DMAPS at the near-surface for all
283 membranes.

Membrane ID	C (%)	Cl (%)	O (%)	N (%)	S (%)	X^{DMAPS} (%)
M1-0min	66.49	33.01	0.50	-	-	-
M2-30min	81.78	11.86	5.87	0.25	0.24	23.69
M3-60min	70.54	11.10	16.07	1.16	1.13	25.77
M4-90min	84.52	6.74	8.28	0.20	0.26	26.39

284

285

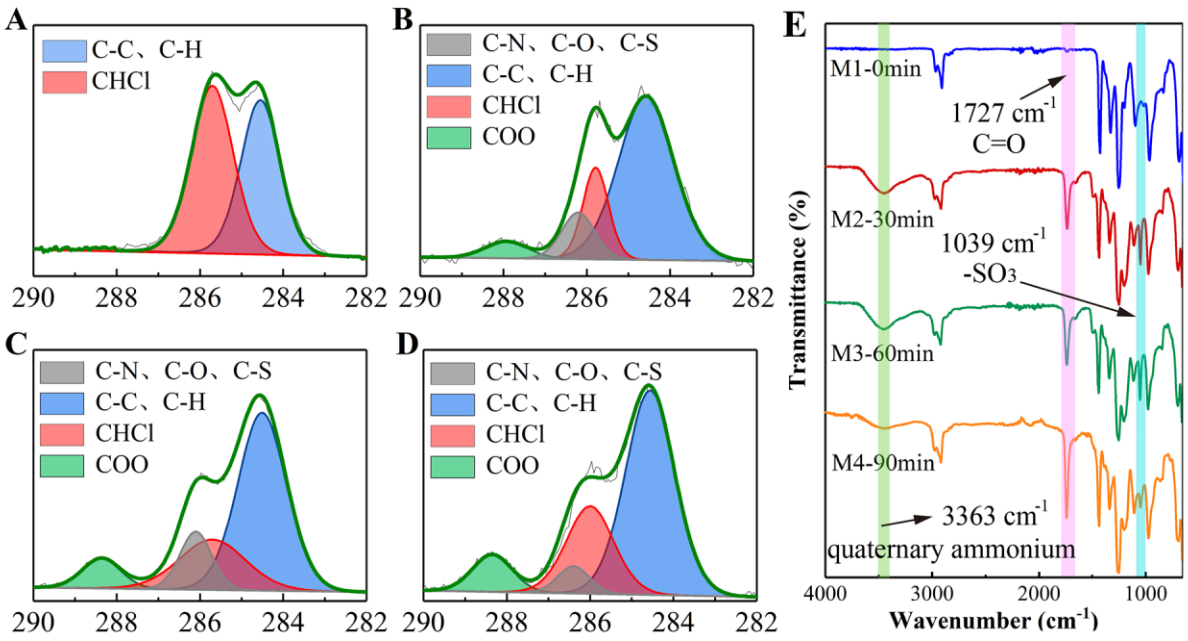

Fig. 3. C 1s peak curve-fitting of XPS spectra for M1-M4: (A) M1-0 min, (B) M2-30min, (C) M3-60 min, (D) M4-90 min. And (E) ATR-FTIR spectra of M1-M4.

3.3. Membrane surface wettability

The behavior of water contact angles on the surface of M1-M4 as a function of time is presented in Fig. 4. Grafting zwitterionic DMAPS to membrane surface decreased the water contact angles and improved the wettability. After a short grafting time of 30 min, the initial contact angle was reduced from 99.2 ± 2.2 ° (M1-0 min) to 89.9 ± 1.9 ° (M2-30 min), and then to 82.4 ± 2.5 ° for M3-60 min. This result is attributed to the strong electrostatic interaction of DMAPS brushes with water molecules [73]. Extending the grafting time to 90 min, the wettability did not further improve, even though higher grafting density and thicker brushes were obtained. We attribute this phenomenon to the influence of the surface roughness. The R_q roughness value of M4-90 min was remarkably larger than that of M3, which may reduce the wetting ability of the membrane surface [74]. Other studies observed similar phenomena [75].

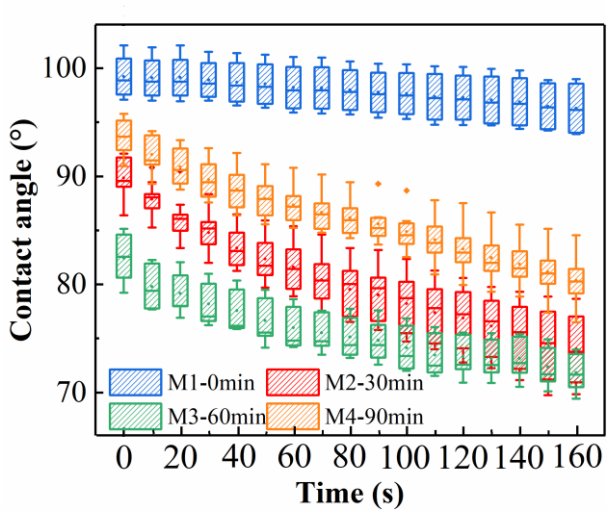

Fig. 4. The behavior of water contact angles on the surface of the membranes as a function of time. For each membrane sample, 4-12 different locations on the surface were detected.

3.4. Transport performance

The permeabilities of M1-M4 are illustrated in Fig. 5A. As also reported by others in the literature, surface grafting reduced the pure water permeability (PWP), likely because the DMAPS brushes obstructed the pores on membrane surface, consistent with the above discussion [22, 71]. The longer the grafting time, the larger the reduction of PWP. Although wettability is an important factor affecting the membrane PWP, the effect of surface morphology was more important in this experiment. However, one should note that even if the PWP was lower for grafted membranes compared to the pristine membrane M1, its values were still high for all the membranes: 2872.3 L $m^{-2} h^{-1} bar^{-1}$ for M2, 2134.1 L $m^{-2} h^{-1} bar^{-1}$ for M3, and 2121.8 L $m^{-2} h^{-1}$ bar^{-1} for M4, thanks to the high performance of the PVC-PolarClean system, the reason of which has been explored and analyzed comprehensively in our previous work [55].

316 The membrane flux recovery ratios (FRR) and SA rejection rates are shown in Fig. 5B. The
317 SA rejection rates were all larger than 93 % because of the small average pore size diameter and
318 narrow pore size distribution (see in Table 1). The average pore diameter of pristine membrane
319 M1-0 min was 18.7 nm, and the SA particle size lies mostly in the range 15-80 nm, on the basis
320 of its molecular weight distribution [76]. Longer grafting time ensured smaller surface pore
321 diameter and surface porosity, thus improved the rejection rate from 93.2 ± 2.4 % (M1), to 96.0
322 ± 2.3 % (M2), 97.0 ± 3.6 % (M3), and 96.4 ± 2.4 % (M4).

323 The anti-fouling property is of vital importance for UF membrane application and the main
324 objective of this study. After the 7-h fouling stage, DI water physical washing for 3 min was
325 employed to assess the membrane anti-fouling behavior. The FRR for pristine M1 was 42.6 ±
326 0.9 %. After surface grafting of zwitterionic DMAPS polymers, the FRR increased significantly.
327 On the one hand, this phenomenon may be attributed to the hydration layer formed around the
328 zwitterionic DMAPS brushes. On the other hand, the foulants were also repelled by polymer
329 brushes because of steric hindrance [17]. It is interesting to note that M2-30 min, even if
330 associated with the shortest investigated grafting time, exhibited an important improvement of
331 FRR (86.4 %), indicating uniform coverage of DMAPS layer on membrane surface, and
332 demonstrating the high efficiency of DMAPS to improve antifouling properties. M3-60 min
333 showed a slightly increased FRR (89.4 %) with respect to M2, but when extending the grafting
334 time to 90 min, the anti-fouling property declined with a FRR of 77.2 %. This phenomenon was
335 consistent with the poor wettability of M4 attributed to the rougher surface. DR_t, DR_r, and DR_{ir}
336 ratios are shown in Fig. S4 (SI).

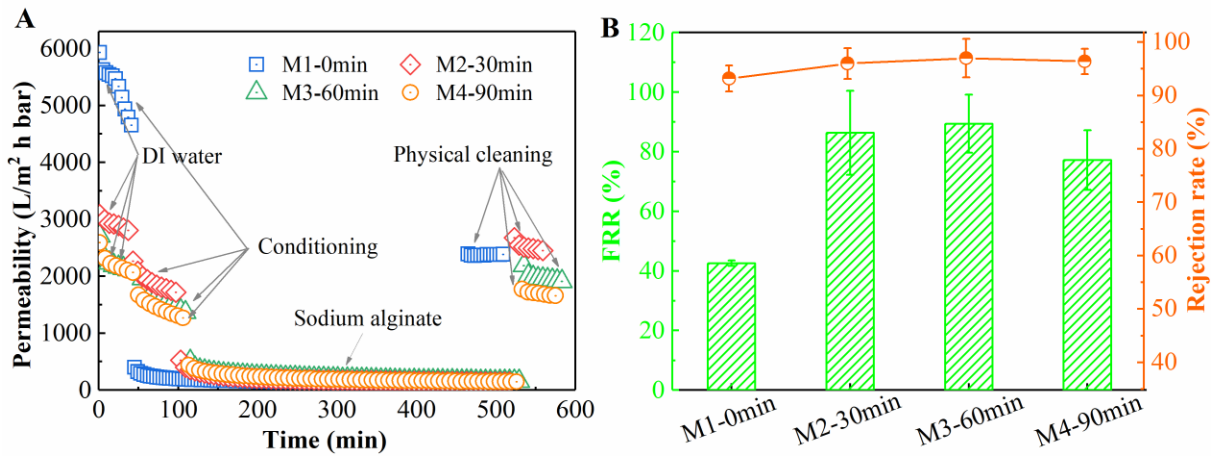

Fig. 5. (A) Permeability with time for M1-0 min, M2-30 min, M3-60 min, and M4-90 min. (B) SA rejection rates and flux recovery ratios (FRR) of M1-M4. The transport performance experiment of every type of membrane was repeated at least twice.

3.5. Membrane-foulant physicochemical interactions

The surface tension parameters of all membranes and model SA particles were estimated from contact angle measurements and are summarized in Table 2. The contact angles of three probe liquids (water, diiodomethane, and formamide) are listed in Table S1. At least 5 measurements for each sample were conducted to acquire the final average contact angle values shown in Table S2. The calculation details are listed in Text S4 (SI). It was found that after surface grafting of zwitterionic DMAPS polymers, the electron acceptor component (γ^+) slightly increased, while the electron donor component (γ^-) increased importantly. This is because that the -SO_3 group of DMAPS is negatively charged in water, and can enhance the electron donating capability, hence the hydrophilicity of the membrane surface [77].

Table 2. The surface tension parameters of all membranes and SA particles.

Item	Surface tension parameters (mJ/m^2)				
	γ^{LW}	γ^-	γ^+	γ^{AB}	γ^{TOT}
M1-0 min	42.028	0.037	0.000	0.011	42.039
M2-30 min	38.448	2.426	0.023	0.477	38.925
M3-60 min	35.821	2.679	0.093	0.997	36.818
M4-90 min	37.866	0.671	0.027	0.267	38.134
SA particles	37.647	9.706	0.669	5.097	42.744

353

354 The interfacial free energy between membrane surface and the SA particles was thus
355 calculated via the surface tension parameters and equations (5-7), and the results are depicted in
356 Fig. 6. The total interaction free energy (ΔG_{132}) is the combination of the Lifshitz−van der Waals
357 (LW) and the Lewis acid−base (AB) interaction energies. A positive value indicates repulsive
358 interaction, while negative value indicates attractive interactions. The more negative is the
359 interaction, the more it is attractive, and the membrane surface is more likely to be fouled or
360 unlikely to be efficiently cleaned after fouling [68, 78]. For M1-M4, their interaction energies
361 with SA particles were all negative, indicating that the SA particles tend to attach on membrane
362 surfaces in all systems. However, after surface grafting of DMAPS, M2-M4 showed a much
363 lowe absolute values of ΔG_{132}, implying the zwitterionic DMAPS polymer brushes effectively
364 reduced the attractive interactions of foulants on the membrane surfaces, thus decreasing the
365 likelihood of foulant attachment and improving membrane anti-fouling properties. Moreover, we
366 found that the Lewis acid−base interaction energy (ΔG_{132}^{AB}) was much more negative than the
367 Lifshitz−van der Waals interaction energy (ΔG_{132}^{LW}), and that the parameter ΔG_{132}^{LW} underwent little
368 change after surface grafting, while ΔG_{132}^{AB} dramatically increased. Therefore, the Lewis

acid−base interaction energy (ΔG_{132}^{AB}) played a key role in the membrane fouling process. In summary, the main mechanism by which DMAPS polymer brushes enhanced the anti-fouling property of the membrane is by increasing the Lewis acid-base interaction energy. The relationship between ΔG_{132} and water contact angle, as well as between ΔG_{132} and FRR values, is presented in Fig. S5 (SI), showing a significant correlation, which indicates the suitable applicability of the XDLVO theory to predict and explain the membrane fouling behavior.

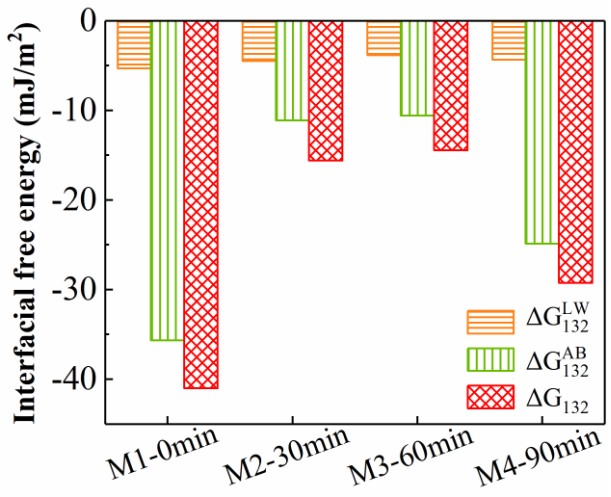

Fig. 6. Total interaction energies (ΔG_{132}), Lifshitz−van der Waals interaction energies (ΔG_{132}^{LW}) and Lewis acid−base (AB) interaction energies (ΔG_{132}^{AB}) between the membranes and SA particles in aqueous solution.

4. Conclusion

On the basis of our previous study [55], green solvent PolarClean was utilized to fabricate PVC membranes with high permeabilities and foulants rejection rates. This work is aimed at improving their anti-fouling properties via environmentally friendly method. Zwitterionic DMAPS polymers were grafted on the membrane surface by ARGET-ATRP method with lower

environment impacts compared to traditional grafting methods. The XDLVO theory revealed that these polymer brushes could significantly reduce the interactions between membrane and foulants, especially those related to hydrophobic effects, thus promoting the membrane anti-fouling property. Other reports typically proposed grafting-based modification by pre-coating the surface with biophenols (*e.g.*, polydopamine, tannic acid) [17, 24, 25, 79-81]. However, this approach dramatically decrease the permeability of UF membranes, while increasing the complexity and cost of membrane fabrication. Instead, our study demonstrate the direct utilization of the chlorine atoms of the membrane backbones as effective initiation sites for the polymerization, greatly improving the anti-fouling performance while retaining membrane high permeability to the maximum extent.

The optimized grafting time was 30 min, and the related membrane exhibited very high performance: pure water permeability of 2872.3 L m^{-2} h^{-1} bar^{-1}, flux recovery rate of 86.4 % after a 7-hour SA fouling phase and foulant particle rejection of 96.0 %. This work achieved both green production and improved membrane performance, representing a successful exploration of sustainable chemistry and engineering toward membrane manufacturing. Further study should be directed to utilize this membrane in wastewater treatment, evaluating its anti-fouling and anti-bacterial properties in practical application.

CRediT authorship contribution statement

Wancen Xie: Investigation, Validation, Formal analysis, Visualization, Data curation, Writing - original draft. **Alberto Tiraferri:** Formal analysis, Writing - review & editing. **Xuanyu Ji:** Validation, Formal analysis, Investigation. **Chen Chen:** Writing. **Yuhua Bai:** Writing. **John C.**

Crittenden: Writing. **Baicang Liu:** Conceptualization, Supervision, Formal analysis, Writing review & editing.

Declaration of competing interest

The authors declare that they have no known competing financial interests or personal relationships that could have appeared to influence the work reported in this paper.

Acknowledgments

This work was supported by the National Natural Science Foundation of China (52070134, 51678377), and Sichuan University and Yibin City People's Government strategic cooperation project (2019CDYB-25). We would like to thank the Institute of New Energy and Low-Carbon Technology, Sichuan University, for SEM-EDS measurement. The authors acknowledge Solvay Specialty Polymers for providing PolarClean.

Appendix A. Supplementary material

The following is the supplementary material related to this article:

Surface tension parameters of probe liquids (Table S1); Contact angles of all membranes and SA foulants (Table S2); Values of pore diameters information for all membranes (Table S3); Ternary phase diagram of PVC with PolarClean, DMAc and NMP used as solvent and DI water as nonsolvent (Fig. S1). SEM images of PVC membrane surface morphologies obtained with different grafting times: 120 min and 180 min (Fig. S2). XPS spectra of PVC membranes obtained with different grafting time (Fig. S3); DR_r, DR_{ir}, and DR_t for all membranes obtained with different grafting time (Fig. S4); (A) Correlation between the total interaction energy (ΔG_{132}) and FRR. (B) Correlation between the total interaction energy (ΔG_{132}) and water contact angles (Fig. S5).

References

[1] Y. Saeki, T. Emura, Technical progresses for PVC production, Prog. Polym. Sci. 27 (2002) 2055-2131.

[2] S. Moulay, Chemical modification of poly(vinyl chloride)—Still on the run, Prog. Polym. Sci. 35 (2010) 303-331.

[3] J. A. Xu, Z. L. Xu, Poly(vinyl chloride) (PVC) hollow fiber ultrafiltration membranes prepared from PVC/additives/solvent, J. Membr. Sci. 208 (2002) 203-212.

[4] Y. Zhang, X. Tong, B. Zhang, C. Zhang, H. Zhang, Y. Chen, Enhanced permeation and antifouling performance of polyvinyl chloride (PVC) blend Pluronic F127 ultrafiltration membrane by using salt coagulation bath (SCB), J. Membr. Sci. 548 (2018) 32-41.

[5] T. Ahmad, C. Guria, A. Mandal, Optimal synthesis and operation of low-cost polyvinyl chloride/bentonite ultrafiltration membranes for the purification of oilfield produced water, J. Membr. Sci. 564 (2018) 859-877.

[6] X. Fan, Y. Su, X. Zhao, Y. Li, R. Zhang, J. Zhao, Z. Jiang, J. Zhu, Y. Ma, Y. Liu, Fabrication of polyvinyl chloride ultrafiltration membranes with stable antifouling property by exploring the pore formation and surface modification capabilities of polyvinyl formal, J. Membr. Sci. 464 (2014) 100-109.

[7] D. Rana, T. Matsuura, Surface Modifications for Antifouling Membranes, Chem. Rev. 110 (2010) 2448-2471.

[8] B. Liu, C. Chen, W. Zhang, J. Crittenden, Y. Chen, Low-cost antifouling PVC ultrafiltration membrane fabrication with Pluronic F 127: Effect of additives on properties and performance, Desalination 307 (2012) 26-33.

[9] Q. Wu, W. Xie, H. Wu, L. Wang, S. Liang, H. Chang, B. Liu, Effect of volatile solvent and evaporation time on formation and performance of PVC/PVC-g-PEGMA blended membranes, RSC Advances 9 (2019) 34486-34495.

[10] S.-Y. Wang, L.-F. Fang, L. Cheng, S. Jeon, N. Kato, H. Matsuyama, Novel ultrafiltration membranes with excellent antifouling properties and chlorine resistance using a poly(vinyl chloride)-based copolymer, J. Membr. Sci. 549 (2018) 101-110.

[11] L. Zheng, J. Wang, D. Yu, Y. Zhang, Y. Wei, Preparation of PVDF-CTFE hydrophobic membrane by non-solvent induced phase inversion: Relation between polymorphism and phase inversion, J. Membr. Sci. 550 (2018) 480-491.

[12] N. Singh, Z. Chen, N. Tomer, S. R. Wickramasinghe, N. Soice, S. M. Husson, Modification of regenerated cellulose ultrafiltration membranes by surface-initiated atom transfer radical polymerization, J. Membr. Sci. 311 (2008) 225-234.

[13] C. J. Porter, J. R. Werber, C. L. Ritt, Y.-F. Guan, M. Zhong, M. Elimelech, Controlled grafting of polymer brush layers from porous cellulosic membranes, J. Membr. Sci. 596 (2020) 117719.

[14] J. F. Hester, P. Banerjee, Y. Y. Won, A. Akthakul, M. H. Acar, A. M. Mayes, ATRP of Amphiphilic Graft Copolymers Based on PVDF and Their Use as Membrane Additives, Macromolecules 35 (2002) 7652-7661.

468 [15] F. Galiano, A. Figoli, S. A. Deowan, D. Johnson, S. A. Altinkaya, L. Veltri, G. De Luca,
469 R. Mancuso, N. Hilal, B. Gabriele, J. Hoinkis, A step forward to a more efficient wastewater
470 treatment by membrane surface modification via polymerizable bicontinuous microemulsion, J.
471 Membr. Sci. 482 (2015) 103-114.

472 [16] Y.-Y. Cheng, C.-H. Du, C.-J. Wu, K.-X. Sun, N.-P. Chi, Improving the hydrophilic and
473 antifouling properties of poly(vinyl chloride) membranes by atom transfer radical polymerization
474 grafting of poly(ionic liquid) brushes, Polym. Adv. Technol. 29 (2018) 623-631.

475 [17] D. M. Davenport, J. Lee, M. Elimelech, Efficacy of antifouling modification of
476 ultrafiltration membranes by grafting zwitterionic polymer brushes, Sep. Purif. Technol. 189
477 (2017) 389-398.

478 [18] W. Chen, Y. Su, J. Peng, X. Zhao, Z. Jiang, Y. Dong, Y. Zhang, Y. Liang, J. Liu, Efficient
479 Wastewater Treatment by Membranes through Constructing Tunable Antifouling Membrane
480 Surfaces, Environ. Sci. Technol. 45 (2011) 6545-6552.

481 [19] J. Jiang, P. Zhang, L. Zhu, B. Zhu, Y. Xu, Improving antifouling ability and
482 hemocompatibility of poly(vinylidene fluoride) membranes by polydopamine-mediated ATRP, J.
483 Mater. Chem. B 3 (2015) 7698-7706.

484 [20] J.-H. Li, M.-Z. Li, J. Miao, J.-B. Wang, X.-S. Shao, Q.-Q. Zhang, Improved surface
485 property of PVDF membrane with amphiphilic zwitterionic copolymer as membrane additive,
486 Appl. Surf. Sci. 258 (2012) 6398-6405.

487 [21] Y.-F. Zhao, P.-B. Zhang, J. Sun, C.-J. Liu, Z. Yi, L.-P. Zhu, Y.-Y. Xu, Versatile
488 antifouling polyethersulfone filtration membranes modified via surface grafting of zwitterionic

polymers from a reactive amphiphilic copolymer additive, J. Colloid Interface Sci. 448 (2015) 380-388.

[22] W.-W. Yue, H.-J. Li, T. Xiang, H. Qin, S.-D. Sun, C.-S. Zhao, Grafting of zwitterion from polysulfone membrane via surface-initiated ATRP with enhanced antifouling property and biocompatibility, J. Membr. Sci. 446 (2013) 79-91.

[23] P.-S. Liu, Q. Chen, X. Liu, B. Yuan, S.-S. Wu, J. Shen, S.-C. Lin, Grafting of Zwitterion from Cellulose Membranes via ATRP for Improving Blood Compatibility, Biomacromolecules 10 (2009) 2809-2816.

[24] C. Cheng, S. Li, W. Zhao, Q. Wei, S. Nie, S. Sun, C. Zhao, The hydrodynamic permeability and surface property of polyethersulfone ultrafiltration membranes with mussel-inspired polydopamine coatings, J. Membr. Sci. 417-418 (2012) 228-236.

[25] H. C. Yang, K. J. Liao, H. Huang, Q. Y. Wu, L. S. Wan, Z. K. Xu, Mussel-inspired modification of a polymer membrane for ultra-high water permeability and oil-in-water emulsion separation, J. Mater. Chem. A 2 (2014) 10225-10230.

[26] D. S. Kim, J. S. Kang, Y. M. Lee, Microfiltration of activated sludge using modified PVC membranes: Effect of pulsing on flux recovery, Sep. Sci. Technol. 38 (2003) 591-612.

[27] J. Seok Kang, S. Hoon Lee, H. Huh, J. Kie Shim, Y. Moo Lee, Preparation of chlorinated poly(vinyl chloride)-g-poly(N-vinyl-2-pyrrolidinone) membranes and their water permeation properties, J. Appl. Polym. Sci. 88 (2003) 3188-3195.

508 [28] A. Siekierka, J. Wolska, W. Kujawski, M. Bryjak, Modification of poly(vinyl chloride)
509 films by aliphatic amines to prepare anion-exchange membranes for Cr (VI) removal, Sep. Sci.
510 Technol. 53 (2018) 1191-1197.

511 [29] L. Zhang, M. Tang, J. Zhang, P. Zhang, J. Zhang, L. Deng, C. Lin, A. Dong, One simple
512 and stable coating of mixed-charge copolymers on poly(vinyl chloride) films to improve
513 antifouling efficiency, J. Appl. Polym. Sci. 134 (2017).

514 [30] J. Dai, Y. Dong, C. Yu, Y. Liu, X. Teng, A novel Nafion-g-PSBMA membrane prepared
515 by grafting zwitterionic SBMA onto Nafion via SI-ATRP for vanadium redox flow battery
516 application, J. Membr. Sci. 554 (2018) 324-330.

517 [31] J. Zhang, J. Yuan, Y. Yuan, X. Zang, J. Shen, S. Lin, Platelet adhesive resistance of
518 segmented polyurethane film surface-grafted with vinyl benzyl sulfo monomer of ammonium
519 zwitterions, Biomaterials 24 (2003) 4223-4231.

520 [32] M. Zhou, H. Liu, J. E. Kilduff, R. Langer, D. G. Anderson, G. Belfort, High-Throughput
521 Membrane Surface Modification to Control NOM Fouling, Environ. Sci. Technol. 43 (2009)
522 3865-3871.

523 [33] J. B. Zimmerman, P. T. Anastas, H. C. Erythropel, W. Leitner, Designing for a green
524 chemistry future, Science 367 (2020) 397-400.

525 [34] L. Liu, H. Chen, F. Yang, Enhancing membrane performance by blending ATRP grafted
526 PMMA–TiO2 or PMMA–PSBMA–TiO2 in PVDF, Sep. Purif. Technol. 133 (2014) 22-31.

527 [35] L. Zhang, Y. Lin, L. Cheng, Z. Yang, H. Matsuyama, A comprehensively fouling- and
528 solvent-resistant aliphatic polyketone membrane for high-flux filtration of difficult oil-in-water
529 micro- and nanoemulsions, J. Membr. Sci. 582 (2019) 48-58.

530 [36] Y.-H. Zhao, K.-H. Wee, R. Bai, A Novel Electrolyte-Responsive Membrane with Tunable
531 Permeation Selectivity for Protein Purification, ACS Appl. Mater. Inter. 2 (2010) 203-211.

532 [37] L.-J. Zhu, F. Liu, X.-M. Yu, A.-L. Gao, L.-X. Xue, Surface zwitterionization of
533 hemocompatible poly(lactic acid) membranes for hemodiafiltration, J. Membr. Sci. 475 (2015)
534 469-479.

535 [38] Y. Zhang, Z. Wang, W. Lin, H. Sun, L. Wu, S. Chen, A facile method for polyamide
536 membrane modification by poly(sulfobetaine methacrylate) to improve fouling resistance, J.
537 Membr. Sci. 446 (2013) 164-170.

538 [39] C. Liu, A. F. Faria, J. Ma, M. Elimelech, Mitigation of Biofilm Development on Thin-
539 Film Composite Membranes Functionalized with Zwitterionic Polymers and Silver
540 Nanoparticles, Environ. Sci. Technol. 51 (2017) 182-191.

541 [40] K. Matyjaszewski, Atom Transfer Radical Polymerization (ATRP): Current Status and
542 Future Perspectives, Macromolecules 45 (2012) 4015-4039.

543 [41] H. Wu, T. Li, B. Liu, C. Chen, S. Wang, J. C. Crittenden, Blended PVC/PVC-g-PEGMA
544 ultrafiltration membranes with enhanced performance and antifouling properties, Appl. Surf. Sci.
545 455 (2018) 987-996.

546 [42] W. Xie, T. Li, C. Chen, H. Wu, S. Liang, H. Chang, B. Liu, E. Drioli, Q. Wang, J. C.
547 Crittenden, Using the Green Solvent Dimethyl Sulfoxide To Replace Traditional Solvents Partly

548 and Fabricating PVC/PVC-g-PEGMA Blended Ultrafiltration Membranes with High
549 Permeability and Rejection, Ind. Eng. Chem. Res. 58 (2019) 6413-6423.

550 [43] P. Krys, K. Matyjaszewski, Kinetics of Atom Transfer Radical Polymerization, Eur.
551 Polym. J. 89 (2017) 482-523.

552 [44] K. Matyjaszewski, Advanced Materials by Atom Transfer Radical Polymerization, Adv.
553 Mater. 30 (2018) 1706441.

554 [45] T. G. Ribelli, M. Fantin, J.-C. Daran, K. F. Augustine, R. Poli, K. Matyjaszewski,
555 Synthesis and Characterization of the Most Active Copper ATRP Catalyst Based on Tris (4-
556 dimethylaminopyridyl)methyl amine, J. Am. Chem. Soc. 140 (2018) 1525-1534.

557 [46] Z. Zhang, X. Wang, K. C. Tam, G. Sèbe, A comparative study on grafting polymers from
558 cellulose nanocrystals via surface-initiated atom transfer radical polymerization (ATRP) and
559 activator re-generated by electron transfer ATRP, Carbohydr. Polym. 205 (2019) 322-329.

560 [47] S. T. Chow, T. L. Ng, The biodegradation of N-methyl-2-pyrrolidone in water by sewage
561 bacteria, Water Res. 17 (1983) 117-118.

562 [48] D. J. C. Constable, P. J. Dunn, J. D. Hayler, G. R. Humphrey, J. L. Leazer, Jr., R. J.
563 Linderman, K. Lorenz, J. Manley, B. A. Pearlman, A. Wells, A. Zaks, T. Y. Zhang, Key green
564 chemistry research areas - a perspective from pharmaceutical manufacturers, Green Chem. 9
565 (2007) 411-420.

566 [49] C. Wang, C. Huang, Y. Wei, Q. Zhu, W. Tian, Q. Zhang, Short-term exposure to
567 dimethylformamide and the impact on digestive system disease: An outdoor study for volatile
568 organic compound, Environ. Pollut. 190 (2014) 133-138.

569 [50] P. Anastas, N. Eghbali, Green chemistry: principles and practice, Chem. Soc. Rev. 39
570 (2010) 301-312.

571 [51] C. Capello, U. Fischer, K. Hungerbuehler, What is a green solvent? A comprehensive
572 framework for the environmental assessment of solvents, Green Chem. 9 (2007) 927-934.

573 [52] F. P. Byrne, S. Jin, G. Paggiola, T. H. M. Petchey, J. H. Clark, T. J. Farmer, A. J. Hunt, C.
574 Robert McElroy, J. Sherwood, Tools and techniques for solvent selection: green solvent
575 selection guides, Sustainable Chem. Processes 4 (2016) 1-24.

576 [53] D. Ji, C. Xiao, S. An, K. Chen, Y. Gao, F. Zhou, T. Zhang, Completely green and
577 sustainable preparation of PVDF hollow fiber membranes via melt-spinning and stretching
578 method, J. Hazard. Mater. 398 (2020) 122823.

579 [54] C. J. Clarke, W.-C. Tu, O. Levers, A. Brohl, J. P. Hallett, Green and Sustainable Solvents
580 in Chemical Processes, Chem. Rev. 118 (2018) 747-800.

581 [55] W. Xie, A. Tiraferri, B. Liu, P. Tang, F. Wang, S. Chen, A. Figoli, L.-Y. Chu, First
582 Exploration on a Poly(vinyl chloride) Ultrafiltration Membrane Prepared by Using the
583 Sustainable Green Solvent PolarClean, ACS Sustainable Chem. Eng. 8 (2020) 91-101.

584 [56] B. M. Pastore, M. J. Savelski, C. S. Slater, F. A. Richetti, Life cycle assessment of N-
585 methyl-2-pyrrolidone reduction strategies in the manufacture of resin precursors, Clean Technol.
586 Environ. Policy 18 (2016) 2635-2647.

587 [57] V. Faggian, P. Scanferla, S. Paulussen, S. Zuin, Combining the European chemicals
588 regulation and an (eco)toxicological screening for a safer membrane development, J. Clean.
589 Prod. 83 (2014) 404-412.

590 [58] H.-Y. Shiu, M. Lee, Y. Chao, K.-C. Chang, C.-H. Hou, P.-T. Chiueh, Hotspot analysis
591 and improvement schemes for capacitive deionization (CDI) using life cycle assessment,
592 Desalination 468 (2019) 114087.

593 [59] B. Simon, K. Bachtin, A. Kiliç, B. Amor, M. Weil, Proposal of a framework for scale-up
594 life cycle inventory: A case of nanofibers for lithium iron phosphate cathode applications, Integr.
595 Environ. Asses. 12 (2016) 465-477.

596 [60] L. Luciani, E. Goff, D. Lanari, S. Santoro, L. Vaccaro, Waste-minimised copper-catalysed
597 azide–alkyne cycloaddition in Polarclean as a reusable and safe reaction medium, Green Chem.
598 20 (2018) 183-187.

599 [61] L. Cseri, G. Szekely, Towards cleaner PolarClean: Efficient synthesis and extended
600 applications of the polar aprotic solvent methyl 5-(dimethylamino)-2-methyl-5-oxopentanoate,
601 Green Chem. 21 (2019) 4178-4188.

602 [62] N. T. Hassankiadeh, Z. Cui, J. H. Kim, D. W. Shin, S. Y. Lee, A. Sanguineti, V. Arcella,
603 Y. M. Lee, E. Drioli, Microporous poly(vinylidene fluoride) hollow fiber membranes fabricated
604 with PolarClean as water-soluble green diluent and additives, J. Membr. Sci. 479 (2015) 204-
605 212.

606 [63] X. Dong, T. J. Jeong, E. Kline, L. Banks, E. Grulke, T. Harris, I. C. Escobar, Eco-friendly
607 solvents and their mixture for the fabrication of polysulfone ultrafiltration membranes: An
608 investigation of doctor blade and slot die casting methods, J. Membr. Sci. 614 (2020) 118510.

609 [64] C. Y. Tang, Y.-N. Kwon, J. O. Leckie, Effect of membrane chemistry and coating layer
610 on physiochemical properties of thin film composite polyamide RO and NF membranes: I. FTIR

611 and XPS characterization of polyamide and coating layer chemistry, Desalination 242 (2009)
612 149-167.

613 [65] Q. Wu, A. Tiraferri, H. Wu, W. Xie, B. Liu, Improving the Performance of PVDF/PVDF-
614 g-PEGMA Ultrafiltration Membranes by Partial Solvent Substitution with Green Solvent
615 Dimethyl Sulfoxide during Fabrication, ACS Omega 4 (2019) 19799-19807.

616 [66] B. Liu, C. Chen, T. Li, J. Crittenden, Y. Chen, High performance ultrafiltration membrane
617 composed of PVDF blended with its derivative copolymer PVDF-g-PEGMA, J. Membr. Sci. 445
618 (2013) 66-75.

619 [67] X. Zhao, Y. Su, W. Chen, J. Peng, Z. Jiang, Grafting perfluoroalkyl groups onto
620 polyacrylonitrile membrane surface for improved fouling release property, J. Membr. Sci. 415
621 (2012) 824-834.

622 [68] C. Liu, D. Song, W. Zhang, Q. He, X. Huangfu, S. Sun, Z. Sun, W. Cheng, J. Ma,
623 Constructing zwitterionic polymer brush layer to enhance gravity-driven membrane performance
624 by governing biofilm formation, Water Res. 168 (2020) 115181.

625 [69] T. Lin, B. Shen, W. Chen, X. Zhang, Interaction mechanisms associated with organic
626 colloid fouling of ultrafiltration membrane in a drinking water treatment system, Desalination
627 332 (2014) 100-108.

628 [70] C. J. van Oss, Acid—base interfacial interactions in aqueous media, Colloids and Surfaces
629 A: Physicochemical and Engineering Aspects 78 (1993) 1-49.

[71] N. Shahkaramipour, A. Jafari, T. Tran, C. M. Stafford, C. Cheng, H. Lin, Maximizing the grafting of zwitterions onto the surface of ultrafiltration membranes to improve antifouling properties, J. Membr. Sci. 601 (2020) 117909.

[72] M. A. U. R. Alvi, M. W. Khalid, N. M. Ahmad, M. B. K. Niazi, M. N. Anwar, M. Batool, W. Cheema, S. Rafiq, Polymer concentration and solvent variation correlation with the morphology and water filtration analysis of polyether sulfone microfiltration membrane, Adv. Polym. Tech. 2019 (2019) 1-11.

[73] J. B. Schlenoff, Zwitteration: Coating Surfaces with Zwitterionic Functionality to Reduce Nonspecific Adsorption, Langmuir 30 (2014) 9625-9636.

[74] C. Meringolo, T. F. Mastropietro, T. Poerio, E. Fontananova, G. De Filpo, E. Curcio, G. Di Profio, Tailoring PVDF Membranes Surface Topography and Hydrophobicity by a Sustainable Two-Steps Phase Separation Process, ACS Sustainable Chem. Eng. 6 (2018) 10069-10077.

[75] Q. Liu, A. A. Patel, L. Liu, Superhydrophilic and Underwater Superoleophobic Poly(sulfobetaine methacrylate)-Grafted Glass Fiber Filters for Oil–Water Separation, ACS Appl. Mater. Inter. 6 (2014) 8996-9003.

[76] W. Shuai, L. Tong, C. Chen, L. Baicang, J. C. Crittenden, PVDF ultrafiltration membranes of controlled performance via blending PVDF-g-PEGMA copolymer synthesized under different reaction times, Front. Environ. Sci. Eng. 12 (2018) 3.

649 [77] H. Wang, M. Park, H. Liang, S. Wu, I. J. Lopez, W. Ji, G. Li, S. A. Snyder, Reducing
650 ultrafiltration membrane fouling during potable water reuse using pre-ozonation, Water Res. 125
651 (2017) 42-51.

652 [78] N. Subhi, A. R. D. Verliefde, V. Chen, P. Le-Clech, Assessment of physicochemical
653 interactions in hollow fibre ultrafiltration membrane by contact angle analysis, J. Membr. Sci.
654 403-404 (2012) 32-40.

655 [79] G. Li, B. Liu, L. Bai, Z. Shi, X. Tang, J. Wang, H. Liang, Y. Zhang, B. Van der Bruggen,
656 Improving the performance of loose nanofiltration membranes by poly-dopamine/zwitterionic
657 polymer coating with hydroxyl radical activation, Sep. Purif. Technol. 238 (2020) 116412.

658 [80] Y. Xu, D. Guo, T. Li, Y. Xiao, L. Shen, R. Li, Y. Jiao, H. Lin, Manipulating the mussel-
659 inspired co-deposition of tannic acid and amine for fabrication of nanofiltration membranes with
660 an enhanced separation performance, J. Colloid Interface Sci. 565 (2020) 23-34.

661 [81] X. Zhang, J. Tian, S. Gao, W. Shi, Z. Zhang, F. Cui, S. Zhang, S. Guo, X. Yang, H. Xie,
662 D. Liu, Surface functionalization of TFC FO membranes with zwitterionic polymers:
663 Improvement of antifouling and salt-responsive cleaning properties, J. Membr. Sci. 544 (2017)
664 368-377.

665